Surface-acoustic-wave single-electron interferometry

Roberta Rodriquez,[1,2,*] Daniel K. L. Oi,[1] Masaya Kataoka,[2] Crispin H. W. Barnes,[2] Toshio Ohshima,[1,3] and Artur K. Ekert[1]
[1]*Centre for Quantum Computation, DAMTP, University of Cambridge, Wilberforce Road, Cambridge CB3 0WA, United Kingdom*
[2]*Cavendish Laboratory, University of Cambridge, Madingley Road, Cambridge CB3 0HE, United Kingdom*
[3]*Fujitsu Laboratories of Europe Ltd. (FLE) Hayes Park Central, Hayes End Road, Hayes, Middlesex UB4 8FE, United Kingdom*
(Received 18 October 2004; revised manuscript received 18 March 2005; published 15 August 2005)

We propose an experiment to observe interference of a single electron as it is transported along two parallel quasi-one-dimensional channels trapped in a single minimum of a traveling periodic electric field. The experimental device is a modification of the surface-acoustic-wave-based quantum processor. Interference is achieved by creating a superposition of spatial wave functions between the two channels and inducing a relative phase shift via either a transverse electric field or a magnetic field. The interference can be used to estimate the decoherence time of an electron in this type of solid-state device.

DOI: 10.1103/PhysRevB.72.085329 PACS number(s): 03.67.−a, 77.65.Dq

Constructing a solid-state single-electron interferometer poses many challenges, especially single-electron transport through the device. Recent experiments on electron interferometers[1,2] and double quantum dots[3] have demonstrated interference, but do not deal with single electrons. These experiments have to take into account many-particle effects, the behavior of electrons as quasiparticles, and the validity of the application of theories such as Fermi liquid theory. In addition to not showing true single particle interference, these factors obscure the fundamental electron coherence time, which is of crucial importance for many prospective solid state quantum information processing schemes.[4–8]

Electron quantization using surface-acoustic waves (SAW), originally studied in the context of current standards,[9,10] has recently lead to a proposal for the implementation of a quantum processor in the solid state that uses this mechanism.[11] Advantages of the proposed SAW devices include the unique feature of creating a completely polarized initial state and of making ensemble measurements over billions of identical computations. Additionally, these systems are similar to quantum dots, but have the advantage that manipulation of qubits can be done with static potentials on surface gates without the need for expensive high-frequency pulse generation.[3] Furthermore, the mechanism of SAW transport eliminates the problem of backscattering from discontinuities in the electron trajectory which also detracts from the ideal interferometry experiment.[12–15] This opens up the range of mechanisms for inducing relative phase shifts required to observe interference fringes.

The acoustoelectric devices we consider in this paper are fabricated on modulation doped GaAs-AlGaAs heterostructures. Because GaAs is a piezoelectric material, applying a radio-frequency potential difference between a pair of interdigitated transducers produces vibrations that propagate through the structure as longitudinal waves (SAWs), which in turn induce an electrostatic potential. The SAWs then travel across the two-dimensional electron gas and through a mesa patterned with surface gates that define two parallel quasi-one-dimensional channels. By altering the static potential on the surface gates it is possible to trap a single electron in each SAW potential minimum in each of the two channels with an accuracy greater than 1 part in 10^5.[16] A two level quantum system (qubit) can be defined by the presence of a single electron in either the lower or the upper channel ($|0\rangle$ and $|1\rangle$, respectively). Single qubit rotations can be implemented by variations in the static potentials defined by surface gates. The probability of the presence of an electron in either channel can be measured directly from the current output of each channel via Ohmic contacts.

A Mach-Zender single particle interferometer can be constructed from a single qubit SAW processor by a combination of σ_x and σ_z gates. The size of the interference fringes gives an indication of the fidelity of device which is a combination of the individual gate fidelities and decoherence. By varying the effective length of the interferometer, the dephasing time of single electrons in this system can be estimated, which is expected to be the limiting factor for coherent manipulation of these systems.

Decoherence of qubit can be characterized by two time scales, the T_1 and the T_2 time, which are a measure of the rate at which the system experiences unwanted transitions and dephasing between quantum levels respectively. In the Bloch sphere picture,[17–19] the T_1 (amplitude damping) time is associated with the contraction of the Bloch sphere along the z axis, in conjunction with a symmetrical contraction along the x and y axes consonant with complete positivity.[20] This transforms a pure state to a completely mixed state. The T_2 (phase relaxation) time is associated with the contraction of the x and y axes only, resulting in a shrinkage of the Bloch sphere to a line along the z axis. In the Markovian regime, an initially pure state $|\psi\rangle=\alpha|0\rangle+\beta|1\rangle$ evolves under phase relaxation as

$$\rho_s(t)=\begin{pmatrix} |\alpha|^2 & \alpha\beta^* e^{-t/T_2} \\ \alpha^*\beta e^{-t/T_2} & |\beta|^2 \end{pmatrix}. \quad (1)$$

The off-diagonal terms (coherences), responsible for interference, decrease in magnitude exponentially, where T_2 is the $1/e$ time constant.

A Mach-Zender interferometer is shown in Fig. 1. Initially, a particle is in the localized state $|0\rangle$ traveling horizontally towards the first beamsplitter. The actions of the beam-

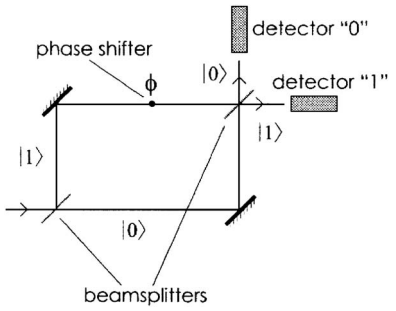

FIG. 1. A Mach Zender interferometer. A single particle at a time is sent horizontally towards the first beamsplitter. We label the state of the particle in the upper and lower arms of the interferometer $|0\rangle$ and $|1\rangle$, respectively. A phase shift is introduced into the upper arm. The two paths are directed to interfere at a second beamsplitter. Particle detectors determine from which direction the particle exits the interferometer.

splitters, having transmittances $t=\cos^2\theta$ and reflectances $r=\sin^2\theta$, and phase shifter can be expressed as unitary operations

$$U_{\mathrm{BS}}=\begin{pmatrix}\cos\theta & \sin\theta\\ e^{i\gamma}\sin\theta & -e^{i\gamma}\cos\theta\end{pmatrix}\quad\text{and}\quad\varphi=\begin{pmatrix}1 & 0\\ 0 & e^{i\phi}\end{pmatrix},$$

respectively. The state may experience dephasing for a period of τ, the transit time between the two beamsplitters. The final state after the second beamsplitter is

$$\rho_{00}=\cos^4\theta+\sin^4\theta+\tfrac{1}{2}\mathrm{v}\sin^2 2\theta\cos(\gamma+\phi),$$

$$\rho_{01}=\rho_{10}^{*}$$
$$=\tfrac{1}{2}e^{-i\gamma}\sin 2\theta[\cos 2\theta+\mathrm{v}e^{i(\gamma+\phi)}-2\mathrm{v}\cos^2\theta\cos(\gamma+\phi)],$$

$$\rho_{11}=\tfrac{1}{2}\sin^2 2\theta[1-\mathrm{v}\cos(\gamma+\phi)],$$

where $\mathrm{v}=e^{-\pi/T_2}$. The probabilities of each detector clicking therefore are

$$P_0=\cos^4\theta+\sin^4\theta+\tfrac{1}{2}\mathrm{v}\sin^2 2\theta\cos(\gamma+\phi),\qquad(2a)$$

$$P_1=\tfrac{1}{2}\sin^2 2\theta[1-\mathrm{v}\cos(\gamma+\phi)].\qquad(2b)$$

By varying ϕ, interference fringes can be observed (Fig. 2). Using the standard definition of visibility $\mathrm{v}=(P_{\max}-P_{\min})/(P_{\max}+P_{\min})$, we find that

$$\mathrm{v}_0=\frac{\mathrm{v}\sin^2 2\theta}{2(\cos^4\theta+\sin^4\theta)},\qquad(3a)$$

$$\mathrm{v}_1=\mathrm{v},\quad\forall\quad\theta.\qquad(3b)$$

Therefore v_1 only depends on the dephasing.

We now describe a procedure for calibrating the beamsplitters so that they are both 50:50. If the beamsplitters have different splitting ratios θ_1 and θ_2, the interference pattern will depend on v and the two angles θ_1 and θ_2, so that

$$P_0=\cos^2\theta_1\cos^2\theta_2+\sin^2\theta_1\sin^2\theta_2$$
$$+2\mathrm{v}\sin\theta_1\sin\theta_2\cos\theta_1\cos\theta_2\cos\xi,$$

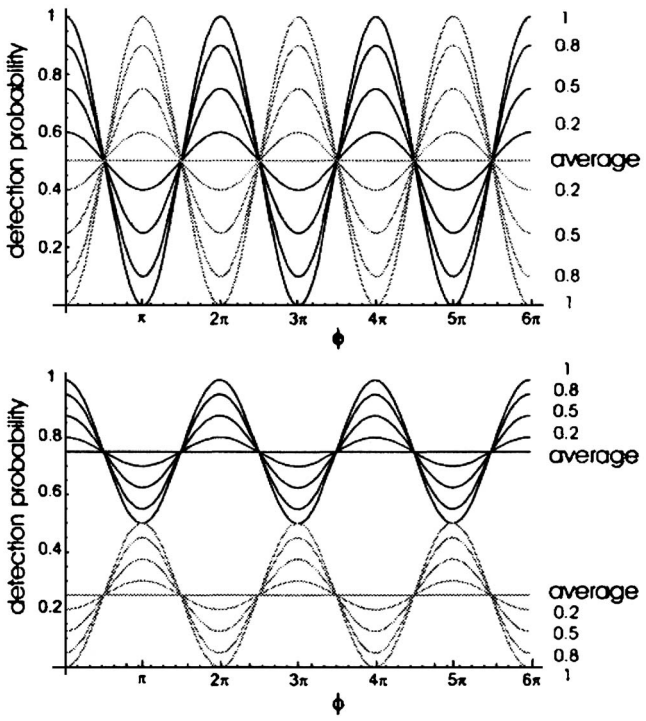

FIG. 2. Interference patterns showing reduction in visibility as decoherence increases, as well as divergence of the two detector curves if the beamsplitter is not 50:50. The upper figure is for $\theta=\pi/4$, the lower one for $\theta=\pi/8$.

$$P_1=1-P_0,$$

where $\xi=\gamma+\phi$. The average values of P_0 and P_1 with respect to ϕ, given by $P(\mathrm{av})=(P_{\max}-P_{\min})/2+P_{\min}$,

$$P_0(\mathrm{av})=\cos^2\theta_1\cos^2\theta_2+\sin^2\theta_1\sin^2\theta_2,$$

$$P_1(\mathrm{av})=1-P_0(\mathrm{av})$$

will be $\frac{1}{2}$ if at least one of the beamsplitter ratios is 50:50.

If initially this is not the case, one can adjust the angle of the first beamsplitter until such a condition is achieved. One can then proceed to adjust the visibilities in general given by

$$\mathrm{v}_0=\frac{2\mathrm{v}\sin\theta_1\sin\theta_2\cos\theta_1\cos\theta_2}{\cos^2\theta_1\cos^2\theta_2+\sin^2\theta_1\sin^2\theta_2},\qquad(4)$$

$$\mathrm{v}_1=\frac{2\mathrm{v}\sin\theta_1\sin\theta_2\cos\theta_1\cos\theta_2}{\sin^2\theta_1\cos^2\theta_2+\cos^2\theta_1\sin^2\theta_2},\qquad(5)$$

where v is the intrinsic visibility of the system. Having calibrated θ_1 to $\pi/4$ we have that $\mathrm{v}_0=\mathrm{v}_1=2\mathrm{v}\cos\theta_2\sin\theta_2$. The value of θ_2 that maximizes v_0 and v_1 is $\theta_2=\pi/4$. When both beamsplitters are 50:50, therefore, v is equal to the visibilities given by the interference patterns. Adjusting the angle of the second beamsplitter until the detected visibilities are maximum therefore calibrates it to a splitting ratio of 50:50.

A two-channel SAW device is shown in Fig. 3. One channel is blocked off so that only one electron is carried in the wavefront of each SAW potential minimum. Information is encoded on the position of the electron, so that localisation to

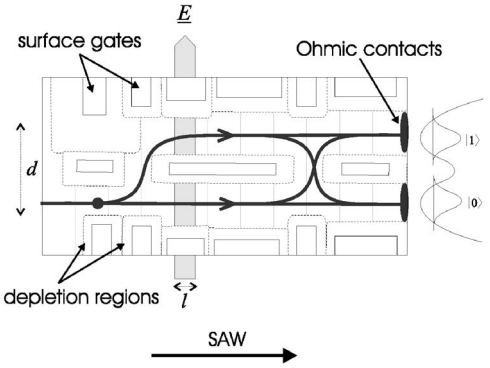

FIG. 3. Single-electron interferometer. A surface acoustic wave propagates from left to right. Single electrons are transported by the SAW along 1D channels defined by surface electrodes parallel to the direction of SAW propagation. By lowering the potential between two channels (by a suitable gap in the surface electrodes), an electron may coherently tunnel laterally like in a beamsplitter. Biasing the channels relative to each other induces a phase gate.

the upper and lower channels corresponds to the qubit states $|0\rangle$ and $|1\rangle$, respectively. A superposition of the two states can be created by lowering the potential barrier between the two channels with the aid of a gap in the surface gates. While the electron is in the region of the gap, it can tunnel between the two channels. Its dynamics can be described by the effective Hamiltonian

$$H = \tfrac{1}{2}\epsilon\sigma_z + \tfrac{1}{2}\Delta\sigma_x, \tag{6}$$

where σ_x and σ_z are the Pauli matrices acting on $|0\rangle$ and $|1\rangle$, and ϵ is the energy splitting between the localized electron energy levels in each well. For small ϵ and for $|\psi(t=0)\rangle = |0\rangle$,

$$|\psi(t)\rangle = \cos(\alpha t)|0\rangle - i\sin(\alpha t)|1\rangle, \tag{7}$$

where $\alpha = \Delta/(2\hbar)$. If the tunneling barrier opened up suddenly it could be characterized directly by a tunneling energy Δ; in a real device, the tunnel barrier opens up gradually so integration over the barrier length is needed in order to determine the effective Δ. The evolution of the state according to this tunneling Hamiltonian only occurs as the SAW carries the electron through this region, so that the tunneling time is determined by the velocity of the SAW and the length of the tunneling region. If we now rewrite Eq. (7) as the map $|0\rangle \mapsto \cos\theta|0\rangle - i\sin\theta|1\rangle$, it is evident that the tunneling region acts, in fact, similarly to a beamsplitter, with the beamsplitter angle θ depending on Δ, the length of the tunneling region, and the SAW velocity.

In order to observe single-electron interference, we introduce a relative phase shift ϕ between the two paths which can be achieved in several ways. One can induce an asymmetry in the double well potential by means of a transverse electric field, as shown in Fig. 3, or by narrowing the 1D-channel confinement potential. Alternatively, one could employ the Aharonov-Bohm effect, which has already been observed in GaAs/AlGaAs heterostructure devices.[21]

Introducing an asymmetry to the double well potential via a transverse electric field separates the eigenstates of the systems into localized single particle eigenfunctions, evolving with different energies:

$$|\psi\rangle = \cos\theta e^{-iE_0 t/\hbar}|0\rangle - i\sin\theta e^{-iE_1 t/\hbar}|1\rangle. \tag{8}$$

The relative phase difference between the two paths is therefore given by the energy difference $\epsilon = E_0 - E_1$ between the two localized states

$$\Delta\phi = \epsilon = \frac{e}{\hbar}\int V\,dt, \tag{9}$$

where V is the voltage difference between the two channels and e is the electronic charge. Since the electrons are transported by the SAW, $\int dt = \tau = l/v$ where l is the length of the channel region experiencing the electric field and v is the velocity of the SAW ($\sim$2700 m/s in GaAs). We can then rewrite Eq. (9) as

$$\Delta\phi = \frac{e|\vec{E}|d}{\hbar}\frac{l}{v}, \tag{10}$$

since $V = \vec{E}\cdot\vec{d}$, where $\vec{E}$ is the the electric field and $\vec{d}$ is the displacement between the two channels, and therefore explicitly calculate $\Delta\phi$.

The lowest electron temperature achievable in a ^{3}He-^{4}He dilution refrigerator is realistically around 100 mK ($\sim$10 μeV), assuming that microwave heating is minimized. We take this thermal energy as the resolution of the experiment. In order to obtain clearly defined oscillations, the minimum transverse potential change needed for each 2π phase change is $\sim$100 μV, corresponding to a maximum phase gate length of 0.1 μm. We cannot have a longer gate without decreasing the number of readings per fringe, given the voltage resolution due to thermal noise. We also require observation of several periods in order to obtain a good estimate of the visibility.

If the relative phase shift is introduced via the Aharonov-Bohm effect,[22] we have that

$$\Delta\phi = \frac{e}{\hbar}\int \vec{B}\cdot\vec{n}\,dS, \tag{11}$$

where S is the surface enclosed by the two paths of the interferometer. In our setup, in order to obtain a 2π phase shift, if the area enclosed by two paths is of the order of $\sim$0.2 μm^2, a $|\vec{B}|$ field change of the order of $\sim$20 mT is required. Interference of electrons has already been observed in the presence of large magnetic fields in Ref. 1; we thus expect that this small magnetic field should not produce much additional decoherence.

To measure the dephasing rate, we need to subject the superposition of localised electron states to increasing lengths of time and measure for each length the reduction of the visibility. This can be achieved by lengthening the effective path length of the interferometer, as shown in Fig. 4. We require at least five different times to obtain a reasonable estimate of T_2. The longest interferometer transit time should be of the order of $2.3\times T_2$, if we require the minimum visibility to be 10% of the initial visibility. Although absolute estimates the T_2 time do not exist, recent experiments place a

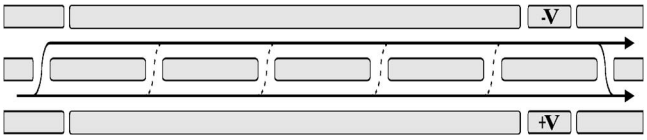

FIG. 4. Configuration for measuring the decoherence rate. By varying the central gate bias, the gaps in the central barrier are opened and closed in such a manner that the path length can be varied, hence varying the time the electron is in superposition between the upper and lower channels.

lower bound on decoherence of ~ 1 ns[3]. Using this value, we find that the longest channel setting needs to be of the order of $v\tau \sim 6$ μm. Increments in channel distance between each setting thus need to be of ~ 1.2 μm or less. This is easily achievable using current electron-beam lithography technology.

The T_1 time, corresponding to unwanted tunneling, can be made extremely long in between the two beamsplitter regions and may be ignored. In the tunneling regions, effects such as scattering from fluctuating impurity potentials (random telegraph noise) do become important. Estimates of the T_2 decoherence time (a lower bound to the $T-1$ time) for similar tunneling regions have been made for a double dot system and found to be at least 1 ns[3]. Since our tunnel regions are ~ 300 nm long, the electron traverses them in a less than 100 ps, so we expect these errors to be small. In any case, these gate errors are constant and thus one can factor out their effect to determine T_2. Since the electron transported by the SAW is shielded from many particle effects, our system may show higher coherence than multielectron quantum dots.[3]

Increasing the channel length to estimate the dephasing time will be a challenge. A main concern will be that the environment of the qubits will change. However, the increase in static impurities will be small (for an average impurity density of ~ 1 μm^{-1}) and techniques exist to "delete" their effects on the qubits, once their presence is located.[23] Calibration of the beamsplitters is vital to eliminate the contribution of mismatched splitting ratios to the variation in interference visibility.

We do not include in our analysis decoherence arising from spin-orbit coupling. This, however, we expect to be negligible because of the much longer decoherence times supported by the spin degree of freedom.[24]

Finally, this device can also be used as an electric field measuring device, since changes in the transverse electric field will result in changes in the interference pattern. By means of a feedback circuit, the absolute size of the field can be measured. This measurement will be subject to shot noise $\sqrt{N}/N = 1\sqrt{N}$, where $N = f\Delta t$ is the total number of electrons collected in time Δt with SAWs of frequency f. There is a trade-off between increased sensitivity, by using a longer Δt, and measurement bandwith.

We would like to thank the Schiff Foundation, Fujitsu, EU projects RESQ (IST-2001-37559) and TOPQIP (IST-2001-39215), Sidney Sussex College and the CMI collaboration for financial support, and Valery Talyanskii for stimulating conversations.

*Electronic address: rr269@damtp.cam.ac.uk

[1] Y. Ji, Y. Chung, D. Sprinzak, M. Heiblum, D. Mahalu, and H. Shtrikman, Nature (London) **422**, 415 (2003).
[2] W. G. van der Wiel, Y. V. Nazarov, S. DeFranceschi, T. Fujisawa, J. M. Elzerman, E. W. G. M. Huizeling, S. Tarucha, and L. P. Kouwenhoven, Phys. Rev. B **67**, 033307 (2003).
[3] T. Hayashi, T. Fujisawa, H. D. Cheong, Y. H. Jeong, and Y. Hirayama, Phys. Rev. Lett. **91**, 226804 (2003).
[4] I. L. Chuang, R. Laflamme, P. W. Shor, and W. H. Zurek, Science **270**, 1633 (1995).
[5] W. G. Unruh, Phys. Rev. A **51**, 992 (1995).
[6] P. W. Shor, Phys. Rev. A **52**, R2493 (1995).
[7] A. Ekert and C. Macchiavello, Phys. Rev. Lett. **77**, 2585 (1996).
[8] A. M. Steane, Phys. Rev. A **68**, 042322 (2003).
[9] J. M. Shilton, V. I. Talyanskii, M. Pepper, D. A. Ritchie, J. E. F. Frost, C. J. B. Ford, C. G. Smith, and G. A. C. Jones, J. Phys.: Condens. Matter **8**, L531 (1996).
[10] V. I. Talyanskii, J. M. Shilton, M. Pepper, C. G. Smith, C. J. B. Ford, E. H. Linfield, D. A. Ritchie, and G. A. C. Jones, Phys. Rev. B **56**, 15 180 (1997).
[11] C. H. W. Barnes, J. M. Shilton, and A. M. Robinson, Phys. Rev. B **62**, 8410 (2000).
[12] P. Bordone, A. Bertoni, M. Rosini, S. Reggiani, and C. Jacoboni, Semicond. Sci. Technol. **19** S412 (2004).
[13] R. Ioniciou, P. Zanardi, and F. Rossi, Phys. Rev. A **63**, 050101(R) (2001).
[14] R. C. Liu, B. Odom, Y. Yamamoto,and S. Tarucha, Nature (London) **391**, 263 (1998).
[15] Numerical studies by Ref. 12 suggest that SAW assisted transport increases quantum coherence over ballistic transport (Refs. 13 and 14) in tunneling regions.
[16] J. Cunningham, V. I. Talyanskii, J. M. Shilton, M. Pepper, A. Kristensen, and P. E. Lindelof, Physica B **280**, 493 (2000).
[17] F. Bloch, Phys. Rev. **70**, 460 (1946).
[18] M. Nielsen and I. Chuang, *Quantum Computation and Quantum Information* (Cambridge University Press, Cambridge, 2000).
[19] D. K. L. Oi, quant-ph/0106035 (unpublished).
[20] K. Kraus, Ann. Phys. (N.Y.) **64**, 311 (1971).
[21] G. Timp, A. M. Chang, J. E. Cunningham, T. Y. Chang, P. Mankiewich, R. Behringer, and R. E. Howard, Phys. Rev. Lett. **58**, 2814 (1987).
[22] Y. Aharonov and D. Bohm, Phys. Rev. **115**, 485 (1959).
[23] R. Crook, A. C. Graham, C. G. Smith, I. Farrer, H. E. Beere, and D. A. Ritchie, Nature (London) **424**, 751 (2003).
[24] J. M. Kikkawa and D. D. Awschalom, Phys. Rev. Lett. **80**, 4313 (1998).